KJO
pISSN: 1011-8942 eISSN: 2092-9382

Korean J Ophthalmol 2016;30(3):206-213
http://dx.doi.org/10.3341/kjo.2016.30.3.206

Original Article

Clinical and Anterior Segment Anatomical Features in Primary Angle Closure Subgroups Based on Configurations of Iris Root Insertion

Ji Wook Hong[1], Sung-Cheol Yun[2], Kyung Rim Sung[1], Jong Eun Lee[1]

[1]*Department of Ophthalmology, University of Ulsan College of Medicine, Seoul, Korea*
[2]*Department of Clinical Epidemiology and Biostatistics, Asan Medical Center, University of Ulsan College of Medicine, Seoul, Korea*

Purpose: To compare the clinical and anterior segment anatomical features in primary angle closure sub-groups based on configurations of iris root insertion.

Methods: Primary angle closure patients were imaged using anterior segment optical coherence tomography. Anterior chamber depth, iris curvature, iris thickness (IT) at the scleral spur and 500, 750, and 1,500 μm from the scleral spur (IT_0, IT_{500}, IT_{750}, and IT_{1500}), lens vault, iris area, angle opening distance (AOD_{500}), angle recess area (ARA_{750}), and trabecular iris space area ($TISA_{750}$) were measured. Iris root insertion was categorized into a non-basal insertion group (NBG) and basal insertion group (BG).

Results: In total, 43 eyes of 39 participants belonged to the NBG and 89 eyes of 53 participants to the BG. The mean age of participants was greater in the NBG than the BG (62.7 ± 5.7 vs. 59.8 ± 7.3 years, $p = 0.043$), and the baseline intraocular pressure was higher in the BG than the NBG (16.4 ± 4.4 vs. 14.9 ± 3.3 mmHg, $p = 0.037$). The BG showed a greater IT_0 (0.265 ± 0.04 vs. 0.214 ± 0.03 mm, $p < 0.001$) and iris area (1.59 ± 0.24 vs. 1.52 ± 0.27 mm^2, $p = 0.045$), lower ARA_{750} (0.112 ± 0.08 vs. 0.154 ± 0.08 mm^2, $p = 0.017$) and AOD_{500} (0.165 ± 0.07 vs. 0.202 ± 0.08 mm, $p = 0.014$) compared to the NBG.

Conclusions: The BG had a narrower anterior chamber angle, thicker peripheral iris, and higher pretreatment intraocular pressure.

Key Words: Anterior segment optical coherence tomography, Anterior segment parameters, Iris root insertion, Primary angle closure

Primary angle closure (PAC) glaucoma is one of the leading causes of blindness, especially in Asian eyes [1-3]. Previous reports have described the anatomical characteristics of eyes with PAC glaucoma, including a short axial length, narrow angles, shallow anterior chamber, and thick lens [4-7]. Previously, the diagnosis of angle closure relied entirely on clinical examination and involved the use of subjective gonioscopic observation. Recent advances in imaging devices have enabled various anterior segment (AS) parameters to be measured. AS optical coherence tomography (AS OCT) provides an image of the entire anterior segment in a single frame and AS parameters may be quantitatively measured using a non-contact method with the patient in a sitting position [8,9]. Of the several AS parameters, iris-related parameters have been examined in recent studies. Wang et al. [10,11] reported that iris curvature (IC), iris area (IA), and iris thickness (IT) were independently associated with a narrow angle. In addition, pe-

Received: July 3, 2015 *Accepted*: July 27, 2015

Corresponding Author: Kyung Rim Sung, MD, PhD. Department of Ophthalmology, Asan Medical Center, University of Ulsan College of Medicine, #88 Olympic-ro 43-gil, Songpa-gu, Seoul 05505, Korea. Tel: 82-2-3010-3680, Fax: 82-2-470-6440, E-mail: sungeye@gmail.com

ripheral IT was recently reported as an important predictor of the outcome of laser peripheral iridotomy [12,13]. Another interesting point is the location of the iris root insertion into the ciliary body. The site of peripheral iris insertion into the ciliary body is very close to the trabecular meshwork, and the location of the iris root insertion may thus affect the anterior chamber angle. By use of AS OCT images, we compare the clinical and anterior segment anatomical features in PAC subgroups based on configurations of iris root insertion.

Materials and Methods

Participants

PAC suspect (PACS) or PAC patients evaluated by one glaucoma specialist (KRS) at the glaucoma clinic of Asan Medical Center, Seoul, Korea, from March 2009 to December 2014, and who met the inclusion criteria described below, were consecutively included in this study based on medical record review. The study was approved by the institutional review board of Asan Medical Center and followed the tenets of the Declaration of Helsinki.

All participants underwent a complete ophthalmic examination, including a medical history review, measurement of best-corrected visual acuity, slit-lamp biomicroscopy, Goldmann applanation tonometry, gonioscopy, funduscopic examination using a 90- or 78-diopter lens, stereoscopic optic disc photography, retinal nerve fiber layer photography, a visual field test (Humphrey field analyzer, Swedish Interactive Threshold Algorithm 24-2; Carl Zeiss Meditec, Dublin, CA, USA), and AS OCT (Visante OCT ver. 2.0, Carl Zeiss Meditec).

PACS and PAC were diagnosed by gonioscopic examination. Eyes with appositional contact between the peripheral iris and the posterior trabecular meshwork of greater than 270° were included in the PACS group [14]. Eyes with an occludable angle (appositional contact between the peripheral iris and the posterior trabecular meshwork of more than 270°) and exhibiting features indicating trabecular obstruction by the peripheral iris were considered to have PAC [14]. Such features included an elevated intraocular pressure (IOP), iris whorling (distortion of radially orientated iris fibers), "glaukomflecken" lens opacity, or excessive pigment deposition on the trabecular surface, but without the development of a glaucomatous optic disc or any visual field change [14]. We combined patients with both PACS and PAC eyes, and defined them as having "angle closure" for our current analysis. Only reliable visual field test results (false-positive errors <15%, false-negative errors <15%, and fixation loss <20%) were included in the analysis. Eyes with peripheral anterior synechiae in the angle were excluded.

We excluded patients with a history or current use of topical or systemic medications that could affect the angle or the pupillary reflex; those with a history of previous intraocular surgery, including cataract surgery, laser trabeculoplasty, laser iridoplasty, and laser iridotomy; and those unable to fixate prior to AS OCT examination. Patients with a history of acute PAC, defined by the presence of ocular or periocular pain, nausea or vomiting, and a history of intermittent blurring of vision with haloes; an IOP of more than 30 mmHg; and the presence of at least three of the following conditions: conjunctival injection, corneal epithelial edema, mid-dilated unreactive pupil, and shallow angle closure, were also excluded [15]. Eyes diagnosed with secondary angle closure, such as those with neovascular or uveitic glaucoma, were also excluded. All eyes were newly diagnosed cases, and AS OCT imaging was performed before starting any glaucoma medication or laser treatment or intraocular surgery.

Gonioscopy

Prior to AS OCT imaging, all patients underwent a slit-lamp examination and gonioscopy, conducted by an independent observer (KRS) who had extensive experience in the performance of such examinations. All eyes were examined using a Sussman lens in a darkened room (0.5 cd/m^2). Both static and dynamic gonioscopy were performed using a Sussman lens, with the eye in the primary gaze position. Indentation gonioscopy was performed to determine whether angle closure was attributable to apposition or to peripheral anterior synechiae. Care was taken to ensure that light did not fall on the pupil during the examinations.

Anterior segment optical coherence tomography imaging

All participants were imaged in terms of the nasal and temporal angles (0° to 180°) using AS OCT (Visante OCT,

ver. 2.0, Carl Zeiss Meditec) operating in the enhanced AS single mode (scan length 16 mm, 256 A-scans). To confirm the consistency of iris root insertion according to pupillary reaction, four sessions using four different standardized lighting conditions (3.25, 100.8, 426, and 1,420 cd/m^2), from dark to light, were performed by a single well-trained operator. The room in which the AS OCT imaging was performed had four-graded lighting conditions controlled by four-leveled switches. Thus, the same four-leveled lighting conditions were provided to all participants. Participants were asked to sit back after imaging and wait for 30 seconds, during which time the lighting conditions were changed. After 30 seconds of adaptation to the new lighting conditions, imaging was resumed. Four images, obtained under four different lighting conditions, were obtained for each participant. Of the four images obtained at each session, images obtained at 3.25 cd/m^2 were used for analysis [16]. The AS parameters in each image were evaluated by an independent examiner (JWH) who was blinded to all other test results and the clinical information of the participants.

All parameters were determined using the Image J software ver. 1.46 (National Institutes of Health, Bethesda, MD, USA). The analyzed parameters are described in Fig. 1. Anterior chamber depth was defined as the distance from the corneal endothelium to the anterior surface of the lens. The scleral spur was defined as the point at which a change in the curvature of the inner surface of the angle wall became apparent, often presenting as an inward protrusion of the sclera [17]. After determination of the scleral spur location, iris thicknesses at the scleral spur (IT_0) and 500, 750, and 1,500 μm from the scleral spur (IT_{500}, IT_{750}, and IT_{1500}) were measured [11]. IA was defined as the cross-sectional area of the iris. The anterior chamber area was defined as the cross-sectional area bordered by the corneal endothelium and anterior surface of the lens and iris. IC was defined as the maximum perpendicular distance between the iris pigment epithelium and the line connecting the most peripheral and most central points of the epithelium [11]. Lens vault was defined as the perpendicular distance between the anterior pole of the crystalline lens and the horizontal line joining the two scleral spurs [18]. Angle opening distances (AOD_{500} and AOD_{750}), which were defined as the linear distance between the point of the inner corneoscleral wall (500 and 750 μm anterior to the scleral spur, respectively) and the iris, were also assessed. The angle recess area (ARA_{750}) was defined as the triangular area formed by the AOD_{750}. The corners of the triangle were the angle recess (the apex), the iris surface, and the inner corneoscleral wall. The trabecular iris space area ($TISA_{750}$) was defined as the trapezoidal area with the following boundaries: anteriorly, the AOD_{750}; posteriorly, a line drawn from the scleral spur perpendicular to the plane of the inner scleral wall to the opposing iris; superiorly, the inner corneoscleral wall; and, inferiorly, the iris surface. The measurement variability of the parameters was checked prior to full analysis by calculating the intra-class correlation coefficients. Intra-examiner intra-class correlation coefficient values for the various AS parameters ranged from 0.933 to 0.951 [19]. The image acquisition procedure and analysis methods have been previously described [19-22].

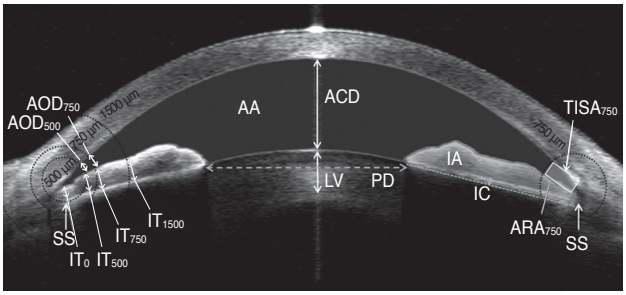

Fig. 1. Anterior segment parameters measured by anterior segment optical coherence tomography and calculated using the Image J software ver. 1.46 (National Institutes of Health, Bethesda, MD, USA). $AOD_{500, 750}$ = angle opening distance; SS = scleral spur; $IT_{0, 500, 750, 1500}$ = iris thickness; AA = anterior chamber area; ACD = anterior chamber depth; LV = lens vault; PD = pupil distance; IA = iris area; IC = iris curvature; $TISA_{750}$ = trabecular iris space area; ARA_{750} = angle recess area.

All parameters except for anterior chamber depth, lens vault, anterior chamber area, and pupillary distance were measured at both the nasal and temporal sides, and an average of the two values was used for the analyses. The iris root insertion configuration was independently assessed by two glaucoma experts (KRS and JEL) who were blind to the other AS OCT parameters and all other test results, including the clinical information of the participants. Four images obtained with different lighting conditions were reviewed by two experts. Iris root insertion was categorized into a non-basal insertion group (NBG) or a basal insertion group (BG), according to the presence of a space between the scleral spur and iris root (Fig. 2A and 2B). Each grader classified each eye as NBG

or BG. If the opinions of the two observers differed, those eyes were excluded.

Statistical analysis

Descriptive analyses of the AS OCT parameters were conducted. Descriptive statistics were calculated to determine the frequencies, means, and standard deviations of each variable. For comparisons of sex ratios and age between the two groups, the chi-square test and unpaired Student's *t*-test, respectively, were used. Comparisons of baseline IOP, spherical equivalent (SE), and pupillary distance between the NBG and BG were performed using linear mixed-effects regression models, which accounted for within-individual associations. Comparisons of all AS OCT parameters between the two groups were performed with the same statistical analysis procedures, which were adjusted for age, sex, eye (right or left eye), SE, and pupillary distance. Residual diagnostic plots were used to detect features of concern in the model. Exploratory analyses of the residuals suggested that the chosen models were appropriate for all of the parameters. All reported *p*-values were two-sided, and a value of $p < 0.05$ was considered statistically significant. SAS ver. 9.2 (SAS Institute Inc., Cary, NC, USA) was used for statistical analyses.

Results

Among the 153 eyes that were qualified by other inclusion criteria, 16 eyes (10.5%) were excluded due to difficult identification of iris root insertion into the ciliary body. In the assessment of iris root insertion, the two experts agreed on the classification (BG or NBG) in 132 of 137 eyes (96.4%). Hence, the final analysis included 132 eyes of 92 individuals. Both eyes within the same participant showed the same grouping in all participants where both eyes qualified. The NBG contained 43 eyes of 39 individuals, while the BG contained 89 eyes of 53 individuals. Mean age (±standard deviation) was significantly greater in the NBG than in the BG (62.7 ± 5.7 vs. 59.8 ± 7.3 years, $p = 0.043$). The baseline IOP was higher in the BG than in the NBG (16.4 ± 4.4 vs. 14.9 ± 3.3 mmHg, $p = 0.037$). The mean SE (1.44 ± 1.13 vs. 0.89 ± 1.1 diopter, $p = 0.053$) and pupillary distance (4.27 ± 0.64 vs. 4.58 ± 0.80 mm, $p = 0.056$) were marginally different between the two groups after accounting for the clustering within-individual effects. The clinical characteristics of the two groups are summarized and compared in Table 1.

The BG showed a greater IT_0 (0.265 ± 0.04 vs. 0.214 ± 0.03 mm, $p < 0.001$), greater IA (1.59 ± 0.24 vs. 1.52 ± 0.27 mm^2, $p = 0.045$), lower ARA_{750} (0.112 ± 0.08 vs. 0.154 ± 0.08 mm^2, $p = 0.017$), and lower AOD_{500} (0.165 ± 0.07 vs. 0.202 ± 0.08 mm, $p = 0.014$) than the NBG. The IC was greater in the NBG than in the BG ($p = 0.031$), but after accounting for pupillary distance and other factors, the level of significance was reduced ($p = 0.075$). AS characteristics of the two groups are compared in Table 2.

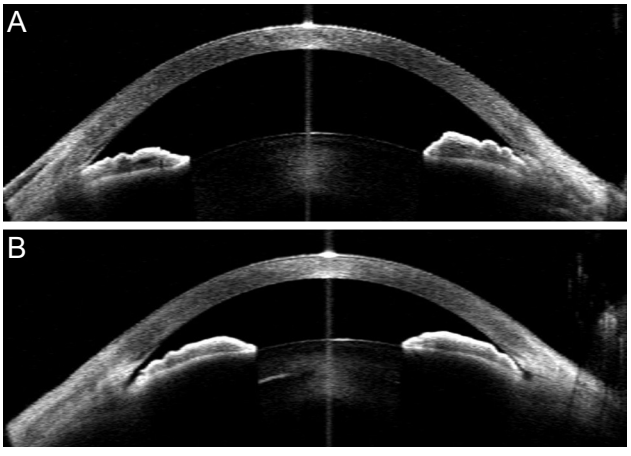

Fig. 2. Location of iris root insertion. (A) Basal insertion and (B) non-basal insertion.

Discussion

Overall, iris insertion was well recognized in most of the AS OCT images in our current study and the second graders showed excellent agreement (96.4%) in terms of eye classification. When both eyes were included, all participants showed a concordant iris insertion shape in the right and left eyes. There is growing evidence that the iris plays an important role in the pathogenesis of angle closure glaucoma [11-13]. In the past, it was not possible to visualize the entire shape of the iris configuration, including the iris cross-sectional area or IT at various locations, or the position of the iris root insertion into the ciliary body. With developments in imaging devices, qualitative or quantitative evaluations of iris characteristics such as this have become feasible. For example, ultrasound biomicroscopy (UBM) has allowed imaging of the entire

Table 1. Comparison of the clinical characteristics of the non-basal iris insertion and basal iris insertion groups in primary angle closure eyes

	NBG	BG	*p*-value
Patient / eye	39 / 43	53 / 89	-
Age (yr)	62.7 ± 5.7	59.8 ± 7.3	0.043
Sex (male / female)	5 / 34	10 / 43	0.438
Spherical equivalent (diopter)	1.44 ± 1.13	0.89 ± 1.11	0.053*
IOP (mmHg)	14.9 ± 3.3	16.4 ± 4.4	0.037*
Pupillary distance (mm)	4.27 ± 0.64	4.58 ± 0.80	0.056*

Values are presented as number or mean ± standard deviation.
NBG = non-basal insertion group; BG = basal insertion group; IOP = intraocular pressure.
*Accounted for the clustering effect within the participant.

Table 2. Comparison of anterior segment optical coherence tomography parameters between the non-basal iris insertion and basal iris insertion groups in primary angle closure eyes

	NBG (n = 43)	BG (n = 89)	*p*-value*	*p*-value†
AA (mm^2)	15.0 ± 2.1	15.7 ± 3.0	0.168	0.786
ACD (mm)	2.10 ± 0.21	2.11 ± 0.30	0.683	0.611
LV	0.982 ± 0.20	0.889 ± 0.25	0.058	0.204
IC	0.354 ± 0.08	0.320 ± 0.08	0.031	0.075
IA (mm^2)	1.52 ± 0.27	1.59 ± 0.24	0.100	0.045
ARA_{750} (mm^2)	0.154 ± 0.08	0.112 ± 0.08	0.033	0.017
$TISA_{750}$ (mm^2)	0.122 ± 0.06	0.099 ± 0.07	0.131	0.063
AOD_{500} (mm)	0.202 ± 0.08	0.165 ± 0.07	0.019	0.014
AOD_{750} (mm)	0.229 ± 0.08	0.239 ± 0.10	0.545	0.863
IT_0 (mm)	0.214 ± 0.03	0.265 ± 0.04	<0.001	<0.001
IT_{500} (mm)	0.302 ± 0.07	0.328 ± 0.07	0.067	0.110
IT_{750} (mm)	0.359 ± 0.07	0.378 ± 0.08	0.225	0.166
IT_{1500} (mm)	0.429 ± 0.06	0.427 ± 0.07	0.913	0.662

Values are presented as mean ± standard deviation.
NBG = non-basal insertion group; BG = basal insertion group; AA = anterior chamber area; ACD = anterior chamber depth; LV = lens vault; IC = iris curvature; IA = iris area; ARA_{750} = angle recess area; $TISA_{750}$ = trabecular iris space area; $AOD_{500, 750}$ = angle opening distance; $IT_{0, 500, 750, 1500}$ = iris thickness.
*Accounted for the clustering effect within the individual; †Accounted for the clustering effect within the individual and adjusted for age, sex, eye, spherical equivalent, and pupillary distance.

iris, and thus several studies that explored iris features have been published [23-26]. Among several iris-related factors, we were interested in the location of the iris root insertion into the ciliary body. The site of iris root insertion into the ciliary body is closely located to the trabecular meshwork and it comprises one part of the anterior chamber angle. Furthermore, the plateau iris configuration, which is considered one of the pathogenetic mechanisms of PAC, especially in Asian eyes, may be related to iris insertion; this is because the plateau iris configuration is defined as an anteriorly directed ciliary body and yields a steep iris root from its point of insertion [27].

Jiang et al. [25] categorized iris insertion into the ciliary body by the use of UBM images. Obviously, UBM shows better images of the ciliary body, but its clinical use is limited because UBM imaging requires ocular contact for image acquisition and should be performed with the patient in the supine position, which may alter the angle configuration. AS OCT has the advantage in this regard,

but due to its poor penetration into tissue, iris insertion into the ciliary body has not been explored using AS OCT imaging. However, the anterior chamber angle is generally well identified with AS OCT, and thus we intended to test the possibility of categorizing the iris root insertion shape using AS OCT imaging. Consequently, PAC eyes could be classified into two groups, NBG and BG. In previous studies, iris root insertion was categorized into basal, middle, and apical groups using UBM [23-25]. However, because AS OCT does not show whole ciliary body features, it was difficult to determine the apical insertion of the iris into the ciliary body. Nonetheless, regardless of whether the iris was inserted into the basal or non-basal portion of the ciliary body, the insertion point was relatively well recognized in most eyes. In a dilated state, the iris root insertion was not differentiated in some eyes, so we acquired four serial images with different lighting conditions and reviewed all four images to determine the location of the iris root insertion. By performing image acquisitions at four light levels, we believe that we reduced the misclassification potential.

Our second goal was to investigate whether the NBG and BG, based on iris root insertion classification, had different clinical and AS anatomical characteristics. Indeed, the BG and NBG individuals showed significant differences in age and baseline IOP. The SE and pupillary distance also showed marginal differences. In other words, patients belonging to the BG were slightly younger and their pre-treatment IOP tended to be higher. Pupil diameter is affected by age [16], and thus the marginal difference in the pupillary distance between the two groups may be partly explained by different age distributions. Some AS OCT parameters showed significant difference between the two groups. IC was greater in the NBG than the BG. AS parameters are greatly influenced by pupil size, so next we adjusted for pupil size and other factors. We subsequently found that the level of significance in the IC was reduced. In contrast, the IA became significant after we accounted for pupil diameter. Generally, an increase in the pupil size (i.e., dilation) resulted in a decrease of the IA. However, our current results showed that the IA difference became more significant when BG individuals had a larger pupil size. Thus, a greater IA, despite an increase in pupil size, seemed to be characteristic of the BG.

After adjusting for age, sex, eye (right or left eye), SE, and pupil size, the basal IT was significantly different between our two study groups. Thus, it seemed that the BG and NBG patients had different shapes in the basal iris configuration, as well as different iris cross-sectional areas. ARA_{750} and AOD_{500} values also showed significant differences, and thus the anterior chamber angle was narrower in the BG. In other words, eyes in the BG had different iris characteristics and a narrower angle than eyes in the NBG. An increased iris volume after pupil dilation or smaller iris cross-sectional area change with physiologic pupil dilation is suggested to be a potential risk factor for PAC [28,29]. Thus, the iris may play a more important role in the pathogenesis of PAC in BG than in NBG eyes. In the meantime, NBG patients were significantly older than those of the BG, a result that partly agreed with a previous report [23]. Because our current study did not evaluate longitudinal changes in iris root configuration, it is difficult to say that aging changes iris root configuration. However, other age-related changes in the AS, such as lens vault or IC changes, would cause the anterior chamber angle to become narrower and thus, those eyes would develop PACS or PAC [8,16]. In this context, the iris may play a more important role in the pathogenesis of PAC in BG cases, and age-related changes in the AS may be more crucial in NBG patients. Since multiple mechanisms are suggested to contribute to the development of PAC, our findings suggest that different mechanisms may play roles in each group with different AS anatomical and clinical characteristics. However, this speculation warrants further evaluation.

Our study had several limitations. First, as mentioned earlier, AS OCT has a limitation in terms of ciliary body visualization due to light penetrance. Thus, it was difficult to accurately define whether the location of the iris insertion was apical or in the middle portion of the ciliary body using this method. Superior and inferior angles often interfered with the eyelid, especially in Asian eyes with a thick eyelid, so iris insertion was assessed at nasal and temporal angles [17].

In conclusion, by the use of AS OCT, we could categorize angle closure eyes into two groups according to the configuration of the iris root insertion into the ciliary body. These two groups had significantly different clinical characteristics and iris and angle parameters. Based on these clinical characteristics and AS OCT parameters, the BG was found to have a narrower anterior chamber angle and

higher level of pretreatment IOP. The results of laser peripheral iridotomy should be investigated in these two groups in a future study to better understand the contributing mechanism of PAC to each group.

Conflict of Interest

No potential conflict of interest relevant to this article was reported.

References

1. Congdon N, Wang F, Tielsch JM. Issues in the epidemiology and population-based screening of primary angle-closure glaucoma. *Surv Ophthalmol* 1992;36:411-23.
2. Foster PJ, Baasanhu J, Alsbirk PH, et al. Glaucoma in Mongolia: a population-based survey in Hovsgol province, northern Mongolia. *Arch Ophthalmol* 1996;114:1235-41.
3. Foster PJ, Johnson GJ. Glaucoma in China: how big is the problem? *Br J Ophthalmol* 2001;85:1277-82.
4. Lowe RF. Aetiology of the anatomical basis for primary angle-closure glaucoma: biometrical comparisons between normal eyes and eyes with primary angle-closure glaucoma. *Br J Ophthalmol* 1970;54:161-9.
5. Sihota R, Lakshmaiah NC, Agarwal HC, et al. Ocular parameters in the subgroups of angle closure glaucoma. *Clin Experiment Ophthalmol* 2000;28:253-8.
6. George R, Paul PG, Baskaran M, et al. Ocular biometry in occludable angles and angle closure glaucoma: a population based survey. *Br J Ophthalmol* 2003;87:399-402.
7. Aung T, Nolan WP, Machin D, et al. Anterior chamber depth and the risk of primary angle closure in 2 East Asian populations. *Arch Ophthalmol* 2005;123:527-32.
8. Cheon MH, Sung KR, Choi EH, et al. Effect of age on anterior chamber angle configuration in Asians determined by anterior segment optical coherence tomography: clinic-based study. *Acta Ophthalmol* 2010;88:e205-10.
9. Kim DY, Sung KR, Kang SY, et al. Characteristics and reproducibility of anterior chamber angle assessment by anterior-segment optical coherence tomography. *Acta Ophthalmol* 2011;89:435-41.
10. Wang BS, Narayanaswamy A, Amerasinghe N, et al. Increased iris thickness and association with primary angle closure glaucoma. *Br J Ophthalmol* 2011;95:46-50.
11. Wang B, Sakata LM, Friedman DS, et al. Quantitative iris parameters and association with narrow angles. *Ophthalmology* 2010;117:11-7.
12. Sung KR, Lee KS, Hong JW. Baseline anterior segment parameters associated with the long-term outcome of laser peripheral iridotomy. *Curr Eye Res* 2015;40:1128-33.
13. Lee RY, Kasuga T, Cui QN, et al. Association between baseline iris thickness and prophylactic laser peripheral iridotomy outcomes in primary angle-closure suspects. *Ophthalmology* 2014;121:1194-202.
14. Foster PJ, Buhrmann R, Quigley HA, Johnson GJ. The definition and classification of glaucoma in prevalence surveys. *Br J Ophthalmol* 2002;86:238-42.
15. Lee KY, Rensch F, Aung T, et al. Peripapillary atrophy after acute primary angle closure. *Br J Ophthalmol* 2007;91:1059-61.
16. Lee Y, Sung KR, Na JH, Sun JH. Dynamic changes in anterior segment (AS) parameters in eyes with primary angle closure (PAC) and PAC glaucoma and open-angle eyes assessed using AS optical coherence tomography. *Invest Ophthalmol Vis Sci* 2012;53:693-7.
17. Sakata LM, Lavanya R, Friedman DS, et al. Assessment of the scleral spur in anterior segment optical coherence tomography images. *Arch Ophthalmol* 2008;126:181-5.
18. Nongpiur ME, He M, Amerasinghe N, et al. Lens vault, thickness, and position in Chinese subjects with angle closure. *Ophthalmology* 2011;118:474-9.
19. Baek S, Sung KR, Sun JH, et al. A hierarchical cluster analysis of primary angle closure classification using anterior segment optical coherence tomography parameters. *Invest Ophthalmol Vis Sci* 2013;54:848-53.
20. Lee KS, Sung KR, Shon K, et al. Longitudinal changes in anterior segment parameters after laser peripheral iridotomy assessed by anterior segment optical coherence tomography. *Invest Ophthalmol Vis Sci* 2013;54:3166-70.
21. Sun JH, Sung KR, Yun SC, et al. Factors associated with anterior chamber narrowing with age: an optical coherence tomography study. *Invest Ophthalmol Vis Sci* 2012;53:2607-10.
22. Han S, Sung KR, Lee KS, Hong JW. Outcomes of laser peripheral iridotomy in angle closure subgroups according to anterior segment optical coherence tomography parameters. *Invest Ophthalmol Vis Sci* 2014;55:6795-801.
23. Wang YE, Li Y, Wang D, et al. Comparison of iris insertion classification among American caucasian and ethnic Chinese using ultrasound biomicroscopy. *Invest Ophthal-*

mol Vis Sci 2013;54:3837-43.

24. Ku JY, Nongpiur ME, Park J, et al. Qualitative evaluation of the iris and ciliary body by ultrasound biomicroscopy in subjects with angle closure. *J Glaucoma* 2014;23:583-8.
25. Jiang Y, He M, Huang W, et al. Qualitative assessment of ultrasound biomicroscopic images using standard photographs: the liwan eye study. *Invest Ophthalmol Vis Sci* 2010;51:2035-42.
26. Chen HJ, Wang X, Yan YJ, Wu LL. Postiridotomy ultrasound biomicroscopy features in the fellow eye of Chinese patients with acute primary angle-closure and chronic primary angle-closure glaucoma. *J Glaucoma* 2015;24:233-7.
27. Kumar RS, Tantisevi V, Wong MH, et al. Plateau iris in Asian subjects with primary angle closure glaucoma. *Arch Ophthalmol* 2009;127:1269-72.
28. Aptel F, Denis P. Optical coherence tomography quantitative analysis of iris volume changes after pharmacologic mydriasis. *Ophthalmology* 2010;117:3-10.
29. Quigley HA. The iris is a sponge: a cause of angle closure. *Ophthalmology* 2010;117:1-2.